



ELSEVIER

Available online at www.sciencedirect.com

SCIENCE @ DIRECT®

Earth and Planetary Science Letters 218 (2004) 109–122

EPSL

www.elsevier.com/locate/epsl

Great earthquakes and slab pull: interaction between seismic coupling and plate–slab coupling

Clinton P. Conrad*, Susan Bilek¹, Carolina Lithgow-Bertelloni

Department of Geological Sciences, University of Michigan, Ann Arbor, MI 48109, USA

Received 3 July 2003; received in revised form 17 October 2003; accepted 27 October 2003

Abstract

Great earthquakes, the few largest earthquakes that account for most of the Earth's seismic energy release, have occurred at only a few subduction zones around the world. Strong locking, or 'seismic coupling', of the interface between plates at certain subduction zones is often invoked to explain these great earthquakes. Although past studies have correlated strong seismic coupling with a compressional stress environment that is characterized by back-arc compression and caused by trenchward motion of the overriding plate, the consequences of this compressional environment for the tectonic forces that drive global plate motions are not yet clear. To examine these consequences, we compared subduction zone earthquake magnitudes to tectonically constrained estimates of the degree to which each slab transmits its excess weight as a direct pull force on a subducting plate. At seismically uncoupled subduction zones that generate only moderate-sized earthquakes, we find that slabs must transmit nearly their entire upper mantle weight as a pull force on the subducting plate. At seismically coupled subduction zones that produce great earthquakes, however, we find that slabs must be nearly completely detached from their subducting plates. This suggests that slabs subducting in a compressional environment experience stress-induced weakening that prevents the effective transmission of the slab pull force. Convergent mantle flow above a descending slab that becomes decoupled from its surface plate may induce additional surface compression that further locks the subduction zone and leads to additional slab decoupling and detachment. The resulting redistribution of plate-driving forces may be responsible for rapid changes in plate motion.

© 2003 Elsevier B.V. All rights reserved.

Keywords: subduction; seismic coupling; tectonic plate motions; great earthquakes; back-arc stresses; plate-driving motions; slab pull

1. Introduction: plate–slab coupling and seismic coupling

Convection in the Earth's mantle is thought to be driven primarily by the descent of dense slabs of subducted lithosphere [1–3]. In fact, tomographic images of the mantle show that the greatest velocity anomalies in the sub-lithospheric mantle are slab-shaped structures that occur be-

* Corresponding author. Tel.: +1-410-516-7765;
Fax: +1-410-516-7933.

E-mail addresses: cpconrad@umich.edu (C.P. Conrad),
sbilek@ees.nmt.edu (S. Bilek), crfb@umich.edu (C. Lithgow-Bertelloni).

¹ Present address: Department of Earth and Environmental Science, New Mexico Institute of Mining and Technology, Socorro, NM 87801, USA.

neath subduction zones [4–6]. Estimates of mantle density heterogeneity made from these seismic images suggest that subducted slabs form the most prominent density anomalies in the mantle [4–6], and thus provide the greatest energy source for driving mantle flow. Because the motions of the Earth's tectonic plates are generally accepted to be the surface expression of this flow [7], the gravitational pull on dense subducted slabs is also thought to be the primary plate-driving force [8–12].

There are two distinct mechanisms by which slabs can drive plate motions [13], and they can be distinguished by the stresses that act to resist the gravitational pull on the slab's negative buoyancy. First, if the slab's excess weight is supported by the surrounding mantle through viscous stresses acting on the sides of the slab, these viscous stresses will induce flow in the mantle. This flow in turn induces shear tractions on the base of the surface plates, driving both subducting and overriding plates toward subduction zones [2,7,10,11,14–16]. We refer to this component as the 'slab suction' force [13]. If slabs had no inherent strength and could be distinguished from the background mantle only by their greater density, slab suction would be the only plate-driving mechanism.

Because rock strength depends strongly on temperature [17], the cold temperatures that make slabs denser than the background mantle also makes them stiffer. As a result, slabs should maintain some mechanical strength as they descend into the mantle and thus some of their excess weight may be supported from above by guiding stresses transmitted through the slab to the surface plate [13,14,18]. The presence of these guiding stresses has been verified for some slabs by stress inversions of intermediate-depth focal mechanisms [19]. Because they couple the slab directly to the subducting surface plate, these guiding stresses exert a force on the subducting plate that pulls this plate toward the subduction zone. We refer to this direct pull as the 'slab pull' force [13]. Although downward motion of the slab is associated with this slab pull mechanism, the plate forces produced by this flow should be overwhelmed by those produced by the direct pull

force because the weight of the slab is supported by the surface plate instead of by the surrounding mantle.

These two different modes for supporting slabs in the mantle excite patterns of mantle flow with different consequences for plate motions. Although the slab pull force acts directly only on the subducting plate, this mechanism has consequences for other plates as well. In particular, the trenchward motion of the subducting plate that is induced by slab pull generates flow in the mantle that exerts tractions on the base of every other plate. These tractions tend to cause overriding plates to move slowly away from subduction zones [13]. The resulting asymmetrical pattern of plate motions contrasts with the symmetrical pattern predicted for slab suction, and can be used to constrain the relative importance of these two mechanisms. Conrad and Lithgow-Bertelloni [13] showed that both asymmetrical pull from upper mantle slabs and symmetrical suction from lower mantle slabs are required to explain the ratio of subducting to non-subducting present-day plate speeds [13]. This suggests both a strong attachment of upper mantle slabs to subducting surface plates and that lower mantle slabs are detached from those in the upper mantle. This detachment is expected because of the phase transition [20] and the factor of 30 or more viscosity jump [1,21] that occur at 670 km.

The physical attachment between a slab and a subducting plate may also be disrupted at shallower depths in the upper mantle if the slab becomes broken or weakened there [22]. This decoupling of a slab from its surface plate should decrease the downward pull of the slab on the Earth's surface topography and increase the geoid locally [22]. Global studies show that this geoid constraint on plate–slab connectivity requires that deep slabs be detached from surface plates [23]. Although some regional studies confirm this result [22], recent detailed modeling of asymmetrical subduction of the Tonga slab suggests that this slab remains coherent as it descends through the upper mantle [24]. Because the ambiguities and difficulties associated with geoid modeling of asymmetrical subduction are large, geoid studies have not yet constrained the degree or depth of

weakening that slabs may experience as they descend. In addition, different slabs may experience different degrees of weakening as they descend, complicating the interpretation of these studies.

Slabs may become weakened if large stresses are applied to them and if their strength decreases with increasing stress or strain rate [22], as it would if dislocation creep [17] or frictional heating [25,26] apply. Thus, the degree of attachment between a subducting plate and a slab may be diminished if the slab is stressed or experiences significant deformation on its way down. This decoupling will diminish the stresses that support the slab from above and cause the slab to be supported instead by viscous mantle stresses. As a result, frictional resistance to subduction, which can cause slab damage or weakening, may diminish the slab pull force in favor of the slab suction force. This scenario has implications for surface plate motions that can be used to constrain the degree of plate–slab connectivity at each subduction zone.

The fraction of slip between a subducting and an overriding plate that occurs seismically is referred to as the degree of ‘seismic coupling’ between the plates [27]. Variations in seismic coupling between subduction zones have been correlated to the amount of resistance that an overriding plate exerts on a slab [28]. This resistance may be related to, or even controlled by, large-scale tectonic forces that drive the overriding plate either towards or away from the subducting plate, which affects the frictional interaction between these plates [29]. Other factors, such as subducting plate and trench morphology, subducting sediments, and the frictional properties of subducted material, may also impact seismic coupling variations [27,30–34]. Seismic coupling has been correlated with the maximum size of earthquakes that occur at a subduction zone [28,29]; subduction zones that are strongly coupled seismically periodically produce great earthquakes ($M_w > 8.0$) [35] while those that are seismically uncoupled only produce moderate to large earthquakes ($M_w < 8.0$) [28]. While there is no direct correlation between seismic coupling and subduction properties such as the convergence rate or the age of subducting lithosphere [27], subduction

zones that produce great earthquakes, such as those in Chile or Alaska, are typically those that exhibit significant back-arc compression while those that are seismically uncoupled, such as the Marianas, typically display back-arc spreading [28,29]. Both back-arc compression and strong seismic coupling can be attributed to the compression associated with trenchward motion of an overriding plate, while motion of the overriding plate away from the subduction zone leads to back-arc extension and weak seismic coupling [29].

Because seismic coupling is strongly affected by tectonic plate motions around the subduction zone, and because these plate motions are the result of slab suction or slab pull forces acting on plates, we might expect the degree of ‘plate–slab coupling’ at a subduction zone, which affects the partitioning between the slab pull and slab suction forces, to also affect the degree of seismic coupling that occurs at a subduction zone. We look at the relationship between these two types of coupling in this work. While we have used the term ‘plate–slab coupling’ to recall the importance of ‘seismic coupling’ to subduction zone tectonics, it is important to recognize that the two terms refer to interactions between different parts of the subduction zone. The former refers to the degree of attachment between the subducting plate and the slab, while the latter refers to the frictional interaction between the subducting and overriding plates.

2. Estimating plate–slab coupling at subduction zones

To determine the degree of plate–slab coupling at each of 10 major subduction zones (Fig. 1), we first estimate the pull force at each subduction zone that would apply if each slab were fully attached to its subducting plate (Table 1). Because Conrad and Lithgow-Bertelloni [13] found that only slabs in the upper mantle contribute to the slab pull force, we sum the excess weight of all upper mantle slab material that is part of a continuous history of subduction at each subduction zone. We use a model of slab locations [11,36]

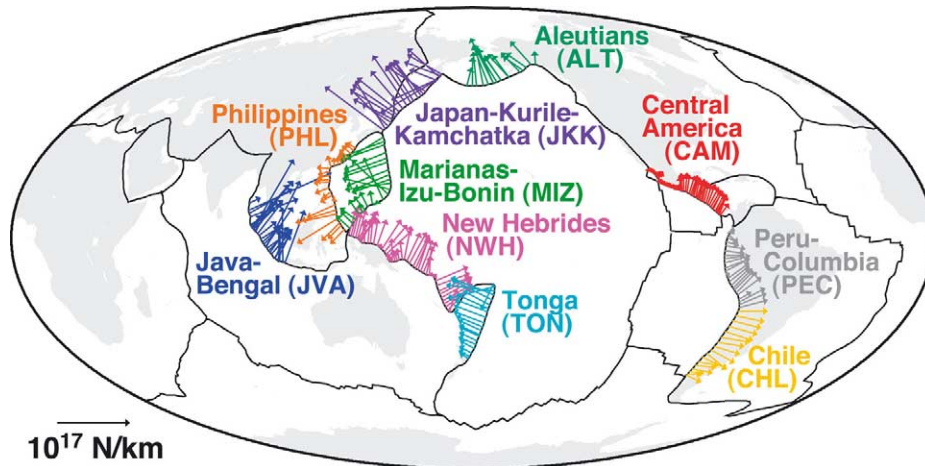


Fig. 1. The magnitude and direction (arrows) of the maximum slab pull force that would apply at each of 10 major subduction zones if the excess weight of all connected upper mantle slab material is transmitted to the subducting plate as slab pull.

that is derived from estimates of Cenozoic and Mesozoic plate motions [11,37]. We then calculate the slab suction forces on each plate from a model of instantaneous mantle flow driven by lower mantle slabs [10,11]. By balancing the slab pull and slab suction plate-driving forces with resisting forces associated with plate-driven viscous mantle flow, we can determine the velocity of each plate in a no-net-rotation reference frame [11].

Predicting plate motions using the above method requires several assumptions. First, we use a radial viscosity structure that produces the best fit to the geoid given our mantle density heterogeneity model [11]. While lateral variations in viscosity cannot be introduced into the spectral determina-

tion of mantle flow that is used here [10,11], we have effectively included mechanically strong slabs, and the toroidal plate motions they produce [38], by introducing a one-sided slab pull force as a plate boundary force [13]. Second, the density heterogeneity model that we use is based on estimates of Cenozoic and Mesozoic plate motions [11] and therefore may contain some discrepancies between modeled and actual slab locations, particularly deeper in the lower mantle where older slabs reside. Misplacement of these older slabs may affect the patterns of plate motions that we predict. Finally, although the ‘ridge push’ force caused by lithospheric thickening is included in the density heterogeneity model that we use and

Table 1
Comparison of subduction zone parameter values

Subduction zone group	Along-strike length (km)	Average pull force (10^{16} N/m)	Pull fraction (%)	Greatest earthquake moment (10^{17} Nm/km)	Harvard CMT moment (10^{17} Nm/km)	Back-arc stress state	Overriding motion (cm/yr)
CAM	3176	1.77	60	5.50	20.2	1.2	0.17
NWH	5628	3.65	67	1.6	20.3	-1.6	2.49
JVA	2396	5.04	100	3.9	5.7	0.0	-1.38
CHL	2587	3.54	40	881	14.3	2.6	0.63
PEC	3351	2.89	73	66.3	24.1	2.0	0.18
TON	3124	4.01	100	18.8	20.1	-2.5	-0.28
MIZ	4451	4.62	100	0.35	2.6	-2.1	-0.71
JKK	2398	6.77	27	204	34.0	1.5	2.17
ALT	2590	4.24	0	517	12.5	0.8	2.04
PHL	3772	2.41	0	3.3	13.1	-0.7	2.19

accounts for about 5–10% of the forces on plates [13], we have not included other forces on plates that are not associated with slabs. These unmodeled forces include those associated with plate–plate interactions at transform faults [39] or continent–continent collisions [40] and can alter plate motions but not drive them because they are not associated with an energy source.

We evaluate a set of predicted plate motions by comparing these predictions with observed present-day plate motions (Fig. 2a), which are obtained [13] from compiled rotation poles for all plates [37] combined with recently updated estimates for the relative motion of Africa and South America [41]. We evaluate each prediction of plate motions by calculating its misfit with observed plate motions. Here we define the total misfit as the area-weighted average magnitude of the vector difference (Fig. 2b,c, right column) between the predicted (Fig. 2b,c, left column) and observed velocity fields (Fig. 2a) measured over a $1 \times 1^\circ$ grid. Predicted velocities are first scaled to produce an average speed equal to that of the observed field. This is permitted because plate speeds depend on the average mantle viscosity [11], which is constrained by postglacial rebound studies, but includes uncertainty of at least a factor of two [21]. The viscosities required for our predicted plate speeds (Fig. 2b,c) to match observed plate speeds (Fig. 2a) are well within this range.

If the total weight of each upper mantle slab is applied at each subduction zone and lower mantle slabs drive plates through slab suction, the average misfit between the observed (Fig. 2a) and predicted (Fig. 2b) plate velocities is 0.5096. This value is a 17% improvement over the misfit of 0.6158 that applies for slab suction operating alone. Some of the remaining misfit can be explained if the degree of plate–slab coupling varies between subduction zones. Specifically, the Japan–Kurile–Kamchatka (JKK) and Aleutian (ALT) slabs may be only partially coupled to the Pacific plate because this plate moves too rapidly toward the north (Fig. 2b, left) if these slabs are pulling with their full capacity, which results in large misfits for the Pacific plate (Fig. 2b, right). Similarly, the stationary motion of South America that re-

sults for fully coupled plates and slabs (Fig. 2b) suggests that the Chilean slab (CHL) may not be completely coupled to the Nazca plate because a detached slab would excite slab suction, which would drive South America westward, as is observed (Fig. 2a).

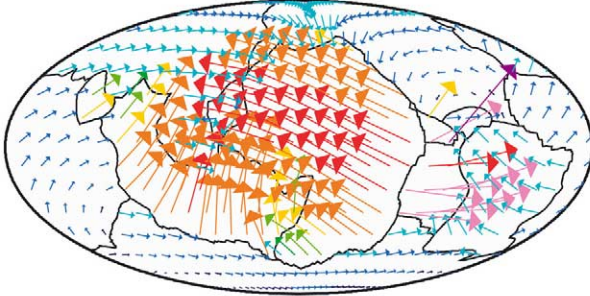
We use a genetic algorithm (Appendix A) to invert for the degree of plate–slab coupling at each subduction zone that produces a set of predicted plate motions (Fig. 2c) that best fits the observed plate motions (Fig. 2a). We find that some slabs, notably MIZ, JVA, and TON, must pull with their entire excess weight (Table 1), indicating strong coupling between these slabs and their subducting plates. The ALT, JKK, and CHL slabs, however, must exhibit weak pull and strong suction (Table 1), suggesting that these slabs are only weakly coupled to their subducting plates. As expected, these changes cause a more westerly motion for both the Pacific and South American plates (Fig. 2c, left), as is observed (Fig. 2a). The remaining average misfit for this solution, which is likely due to modeled plate–plate interactions or errors in the mantle density heterogeneity model, is 0.3675 (Fig. 2c, right), which is a 28% improvement over the model in which the maximum pull force is applied for all slabs (Fig. 2b). Several different genetic algorithm runs produced the same result, as did a simpler ‘slope finding’ iterative inversion technique in which we allowed the fraction of slab pull at each subduction zone to increase or decrease in units of 10% during each iteration if the change improved the misfit. This indicates that our best-fitting solution (Table 1) is indeed a global minimization of the misfit.

3. Comparison with seismic coupling and subduction stresses

The above analysis suggests that some slabs may be better coupled to their subducting plates than others. We explore possible relationships between plate–slab coupling and seismic coupling by examining independent geologic observations. In examining these correlations, it is important to remember that we are comparing estimates of plate–slab coupling to observables that are inde-

a) Observed Velocities

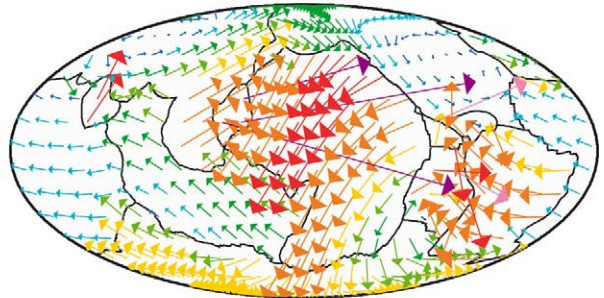
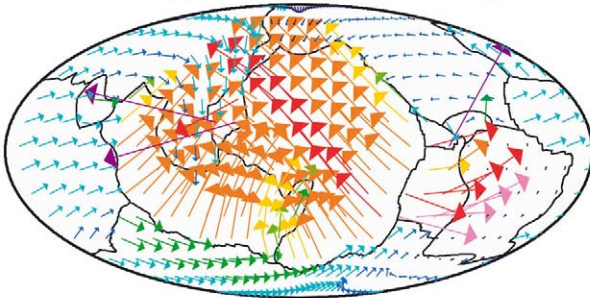
Average Velocity = 3.8 cm/yr



b) Maximum Pull from Upper Mantle Slabs

Average Velocity = 3.3 cm/yr

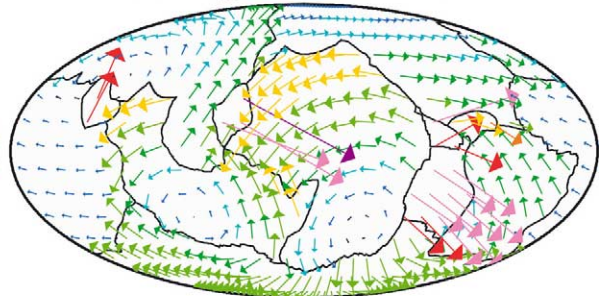
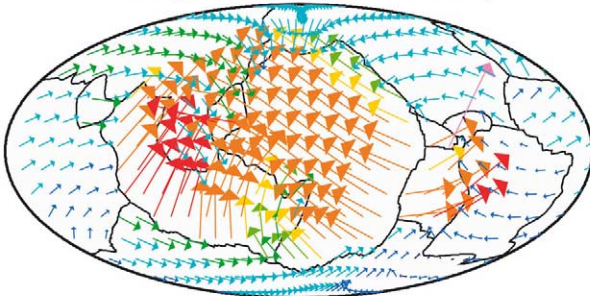
Average Misfit = 0.5096



c) Best-Fitting Pull from Upper Mantle Slabs

Average Velocity = 2.7 cm/yr

Average Misfit = 0.3675



Velocity / Average Velocity

Velocity Misfit

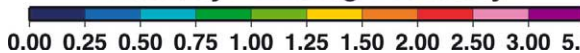


Fig. 2. Comparison of (a) observed plate motions with predictions of plate motions assuming (b) that each upper mantle slab exerts a slab pull force equal to its entire excess weight (pull fraction of 100%) or (c) that the pull from each slab is the fraction of this maximum pull force that produces the best fit to plate motions (variable pull fractions, Table 1). In the left column, colors and arrow lengths indicate plate speeds relative to the average plate speed for that model (given). In the right column these quantities show vector differences between the predicted plate motions and the observed plate motions. The average misfit is the area-weighted average of these vector differences, scaled by the average observed velocity.

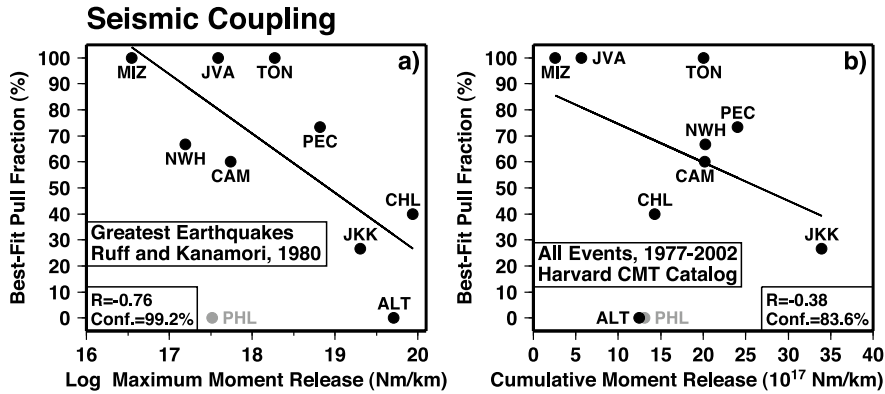


Fig. 3. Comparison between the degree of coupling between a slab and a subducting plate (measured by the best-fit pull fraction) and the degree of seismic coupling between a slab and its overriding plate. Seismic coupling is expressed by (a) the moment release per unit length from the largest events recorded at each subduction zone [28] and (b) the cumulative sum of all shallow (< 100 km) earthquake moments at each subduction zone from the Harvard CMT catalog [44]. The lines drawn are the least-squares best fit to the set of points defined by nine subduction zones (Fig. 1), with the Philippine slab (PHL) excluded because the Philippine plate motion is not well constrained [13], making estimates of PHL plate–slab coupling suspect. Pearson’s correlation coefficient (R) and the one-sided confidence level are included to show that the correlations are not random [42].

pendent of plate–slab coupling, such as seismicity, stress state, and overriding plate motion. Thus, we are essentially testing the forward prediction that the degree of plate–slab coupling is related to these quantities in a predictable way. As a result, we have presented an analysis of the observed correlations (Figs. 3–5) by determining the probability that these correlations are not random. Furthermore, we do not expect perfect correlations here because of the complexity of the sub-

duction process and the difficulty of estimating average values for several of the observables used. Instead, these correlations display basic trends that expose relationships between different controlling parameters.

3.1. Great earthquakes

Because diminished plate–slab coupling may be related to increased frictional resistance to sub-

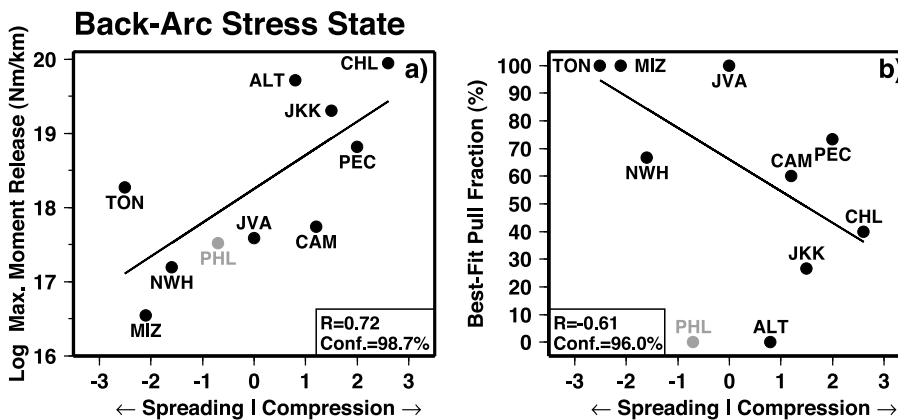


Fig. 4. Comparison between stresses in the back-arc, measured on a relative scale according to Jarrard [45], and both (a) the degree of seismic coupling, measured by the magnitude of the largest events at each subduction zone [28], and (b) the degree of coupling between a slab and a subducting plate (measured by the best-fit pull fraction). The least-squares fit and the statistics of these relationships are given as in Fig. 3.

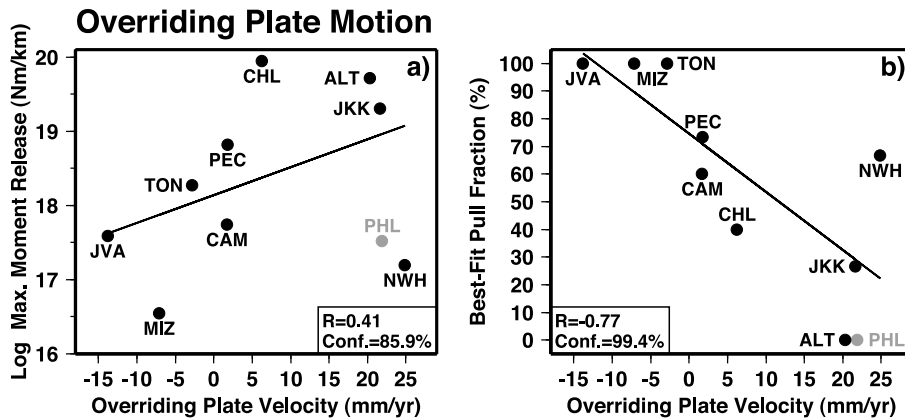


Fig. 5. Similar to Fig. 4, but showing a comparison between average overriding plate velocity, measured normal to the trench (positive is trenchward), and both (a) the degree of seismic coupling and (b) the degree of plate–slab coupling.

duction, we compare the best-fit fraction of slab pull to the degree of seismic coupling at each subduction zone. This quantity can be approximated by the seismic moment released by the largest earthquake at that subduction zone, which typically dominates cumulative estimates of the total seismic moment release [28]. Using the largest-magnitude earthquakes between 1904 and 1976 at the major subduction zones defined by Ruff and Kanamori [28], we assign a maximum seismic moment to each subduction zone group defined here (Fig. 1). Because our tectonically defined subduction zone groups tend to be longer than those defined in this catalog [28], we obtain a maximum moment release per unit length (Table 1) by summing the catalog earthquakes that fall along our subduction zones and dividing by the along-strike length of each subduction zone. Earthquakes from the 1980 catalog used here are presently the largest earthquakes recorded for each subduction zone except for the 2001 $M_w = 8.4$ Peru earthquake, which is larger in magnitude than the previous $M_w = 8.2$ event [28].

We compare the maximum seismic moment released at each subduction zone to the best-fit fraction of slab pull (Fig. 3a). As predicted, the relationship is an inverse one, with the strongest plate–slab coupling occurring at subduction zones that lack large events (Marianas–Izu–Bonin, Java–Bengal, and Tonga) and the weakest plate–slab coupling in regions of great earthquakes (Aleutians, Japan–Kurile–Kamchatka, and Chile). Sub-

duction zones with intermediate plate–slab coupling (Central America, Peru–Columbia, and New Hebrides) do not generate the smallest or the largest maximum earthquake magnitudes. These trends suggest that increased seismic coupling is associated with decreased plate–slab coupling at subduction zones. An exception is the Philippine slab, which does not release great earthquakes but our inversion suggests poor plate–slab coupling (Fig. 3a). The degree of plate–slab coupling for the Philippine slab (PHL) is not well constrained, however, because the motion of the Philippine plate to which it is attached is not well known [13]. Recent geodetic estimates of Philippine plate motion show strong westward motion [43], which is predicted by models with some degree of pull from the Philippine slab (Fig. 2b). An intermediate coupling of the Philippine slab to the Philippine plate would bring PHL close to the trend defined by the other slabs (Fig. 3a).

3.2. Cumulative seismic moment release

When summed over a sufficient amount of time, the cumulative seismic moment provides a more accurate measure of the strength of frictional resistance at a subduction zone, and thus may be a better indicator of seismic coupling [28]. Global catalogs of seismic moment release for a large range of earthquake sizes, such as the Harvard Centroid Moment Tensor (CMT) catalog [44], provide consistent data for the past quarter cen-

tury. Because this time period does not encompass an entire earthquake cycle, as evidenced by the few occurrences of great earthquakes during the past 25 years compared to earlier in the century, the cumulative seismic moment released during this time can be seen to measure a background level of seismicity. We calculated the cumulative seismic moment release per unit length of subduction zone (Table 1) by summing the moment of shallow (less than 100 km) earthquakes in the Harvard CMT catalog [44] from 1977 to June 2002 within a box enclosing each subduction zone, and dividing by the subduction zone's length. This quantity may also be related to the degree of frictional resistance at subduction zones, and a comparison to the best-fit pull fraction (Fig. 3b) shows a roughly inverse relationship similar to the one found for the greatest earthquake moment release (Fig. 3a). In fact, the relative amplitudes of both measures of seismic moment are similar for all slabs (Fig. 3a,b) with the exception of the Aleutians (ALT) and Chile (CHL), which produced the two largest earthquakes ever recorded (1964 $M_w=9.2$ Alaska and 1960 $M_w=9.5$ Chile). These two earthquakes may account for the difference between these two measures of moment because they are included in the maximum moment compilation (Fig. 3a) but not the cumulative one (Fig. 3b). Trends for the great earthquake catalog (maximum moment, Fig. 3a) and the Harvard catalog (cumulative moment for only last 25 years, Fig. 3b) differ in detail and in correlation coefficient, which may be related to the short time covered by the Harvard catalog. However, the overall inverse relationship between seismic moment release and slab pull is clear in both comparisons.

3.3. Back-arc extension or compression

Seismic coupling between a slab and an overriding plate increases if the two push against each other strongly [28]. The compressional environment that results should be evident in the overriding plate's back-arc region [29]. We obtain a relative measure of back-arc stresses (Table 1) by taking the length-weighted average of estimates of this quantity made by Jarrard [45],

who compiled regional geologic indicators of the degree of compression or extension for many smaller subduction zones. We scale these stresses so that neutral stresses have a value of zero. A comparison of these stresses to the seismic moment release from the greatest earthquakes (Fig. 4a) indicates that increased compression in the back-arc region is associated with increased seismic coupling of a subduction zone. Because seismic coupling and plate–slab coupling are inversely related, the comparison of plate–slab coupling to the back-arc stress state (Fig. 4b) shows that a more compressional stress environment is also associated with decreased coupling between a subducting plate and its slab. Thus, the Marianas–Izu–Bonin, Java–Bengal, and Tonga subduction zones, which exhibit an extensional stress environment, also exhibit weak seismic coupling (Fig. 4a) and strong plate–slab coupling (Fig. 4b). On the other hand, the Aleutians, Japan–Kuril–Kamchatka, and Chilean subduction zones show that a compressional stress state is associated with strong seismic coupling (Fig. 4a), weak plate–slab coupling (Fig. 4b), and impeded transmission of pull stresses.

3.4. Overriding plate velocity

The degree of contact between a slab and an overriding plate may depend on the large-scale tectonic or convective stresses that act on these plates. Thus, strong seismic coupling should result if an overriding plate moves toward a subduction zone in an absolute reference frame [29]. Ruff and Kanamori [28] confirmed this prediction by showing that seismic coupling increases if the forces that drive a subducting plate into a subduction zone are greater than those that pull the resulting slab downward into the mantle. Pacheco et al. [27], however, find no correlation between overriding plate velocity and seismic coupling. We calculated the length-weighted average overriding plate velocity normal to the trench along the strike of each subduction zone (Table 1, positive is trenchward). We find that seismic coupling increases as the motion of the overriding plate becomes directed more strongly toward the subduction zone (Fig. 5a). Thus, the compressional

environment that causes both back-arc compression and strong seismic coupling may be caused by the motion of an overriding plate toward the slab subducting beneath it [29] (Fig. 6a). We obtain a similar correlation between overriding plate velocity and Pacheco et al.'s [27] measure of seismic coupling if we combine Pacheco et al.'s [27] subduction zones into the subduction zone groups used here (Fig. 1). Pacheco et al. [27] probably did not observe this correlation because their 19 subduction zones are short enough to express the significant along-strike variations in seismic cou-

pling that are averaged out in our group of 10 longer subduction zones.

We find that trenchward motion of the overriding plate is also associated with poor transmission of the slab pull force (Fig. 5b). This trend is perhaps expected because we have inverted for the set of pull fractions that best fits the observed plate velocities. However, plate–slab coupling should be reduced by trenchward overriding plate motion because this motion increases seismic coupling (Fig. 5a), which is associated with decreased plate–slab coupling (Fig. 3). Converse-

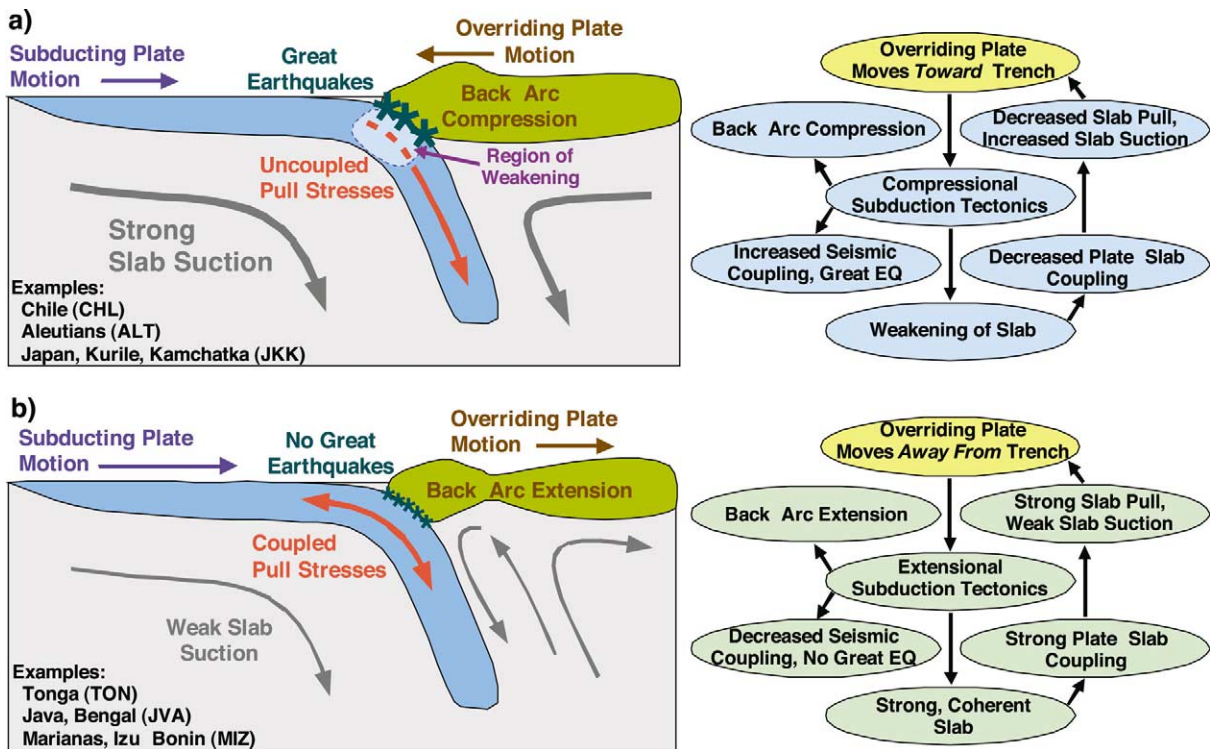


Fig. 6. Cartoons showing the two end-member styles of subduction that are described here (left side) and flow charts that show the inter-relationship of the various subduction properties that define these two styles (right side). If the motion of the overriding plate is toward the subduction zone, as in panel a, the overriding plate is driven into the subducting slab. This compressional environment results in back-arc compression and strong seismic coupling that is expressed by the release of great earthquakes. We find that slab pull at these subduction zones is small, indicating that the slab is weakened by the compressional stresses that are exerted on it by the overriding plate. This weakening diminishes the slab's ability to transmit the gravitational pull on the slab to the subducting plate. Instead, the slab is poorly coupled to the subducting plate and drives plate motions via slab suction, which tends to push the overriding plate even more rapidly toward the trench. Alternatively, if the motion of the overriding plate is away from the subduction zone, as in panel b, the seismic coupling between the slab and the overriding plate will be small, resulting in a more extensional environment characterized by back-arc extension, moderate-sized earthquakes, and low total seismic moment release. Because the slab moves smoothly into the mantle, slabs of this type are well coupled to subducting plates, which allows guiding stresses to transmit the gravitational pull on the slab as a boundary force on the subducting plate. The plate motions driven by this slab pull force contribute to the extensional tectonics of the subduction zone.

ly, overriding plate motion away from the subduction zone decreases seismic coupling (Fig. 5a) and allows strong plate–slab coupling (Fig. 5b) and effective transmission of the slab pull force (Fig. 6b). One exception may be the New Hebrides slab (NWH), which exhibits weak seismic coupling (Fig. 5a), and intermediate plate–slab coupling (Fig. 5b), despite having the fastest overriding plate motion toward the subduction zone. In this case, however, the overriding plate may be broken into several smaller plates [46,47] that shield the slab from the compression associated with trenchward motion of the Pacific plate. This lack of compression is evident in the strong back-arc spreading observed for this subduction zone (Fig. 4).

4. Discussion and conclusions

Previous studies have suggested that overriding plate motion toward a subduction zone generates a compressional stress environment at the subduction zone that leads to back-arc compression, strong seismic coupling, and great earthquakes [28,29]. In this study, we build upon this previous work by showing that this compressional stress environment is also associated with a weak slab pull force acting on the subducting plate (Fig. 6a). In addition, we have demonstrated that a strong slab pull force is typically present at subduction zones operating in a more extensional stress environment typified by overriding plate motion away from the trench, weak seismic coupling, no great earthquakes, and back-arc extension (Fig. 6b).

The association of a compressional stress environment with a diminished slab pull force implies that stresses exerted on the slab by the overriding plate can deform or weaken the slab sufficiently to diminish the transmission of guiding stresses within the slab (Fig. 6a). Such decoupling of a slab from its surface plate may result from a decrease in the slab's effective viscosity by only one to two orders of magnitude [24]. Increased compressive stresses acting on the slab can easily cause such weakening if the slab's rheology is controlled by dislocation creep [17] or if these stresses cause

additional viscous dissipation that generates frictional heating [25,26]. In addition, if frictional resistance to subduction slows the subducting plate sufficiently, the mantle slab may partially detach and descend under its own weight [48]. On the other hand, our results also imply that in the absence of these compressional stresses, a slab will remain sufficiently intact and strong enough to support its own upper mantle weight, which may require maintenance of up to 500 MPa of extensional stress [13].

The degree of coupling between a slab and a subducting plate may also influence global-scale plate-driving forces. If a compressional stress environment weakens the transmission of the slab pull force, then subducted material drives nearby plates instead by exciting the slab suction mechanism [13]. Because this plate-driving mechanism operates symmetrically on both overriding and subducting plates, it will tend to draw both plates toward the subduction zone while at the same time exerting little direct downward force on the downgoing slab. This set of forces tends to draw the overriding plate toward the slab to an even greater degree, thus increasing seismic coupling at the subduction zone and further decreasing plate–slab coupling (Fig. 6a). This positive feedback could cause some subduction zones to become 'locked' into a state of high seismic coupling and weak plate–slab coupling. These subduction zones, which include the Aleutians, Japan–Kuriles–Kamchatka, and Chile, can be expected to produce great earthquakes. In fact, 13 of the 15 greatest subduction zone earthquakes ever recorded, and the four greatest ones, occurred along these three subduction zone groups [30]. Subduction zones that experience strong plate–slab coupling may also experience a positive feedback (Fig. 6b) in which overriding plates are pushed away from subduction zones by the mantle flow generated by trenchward motion of the subducting plate [13]. This decreases seismic coupling, which further increases plate–slab coupling. These subduction zones, exemplified by the Marianas–Izu–Bonin, Java–Bengal, and Tonga slabs, produce only moderate-sized earthquakes [28].

The feedback associated with locking or un-locking of subduction zones can be initiated by

a change in the degree of seismic coupling between a slab and the plate that overrides it. Increased seismic coupling may result from several factors, including changes to the force balance of subducting or overriding plates [40], decreases in slab dip that result from changes in mantle flow [49], a decrease in the coherency of slab material [26], an increase in the smoothness of subducted sediments [30], or the subduction of seamounts [33]. If seismic coupling is strengthened by one of these mechanisms, weakened plate–slab coupling and increased slab suction would lead to additional locking, and possibly a rapid slowing of the subducting plate. Because it does not require changes in the mantle density field, which evolves over tens of millions of years, this slab-locking feedback mechanism may provide an explanation for the observation that plate motions occasionally change directions and speeds in only a few million years [37,40,50]. For example, the sharp bend in the Hawaiian–Emperor seamount chain could be explained if the Aleutian subduction zone became locked at about 43 Ma. This would rapidly diminish the northward pull of the Aleutian slab on the Pacific plate relative to the westward pull of slabs subducting beneath Asia, changing the plate's direction.

Acknowledgements

This work was partially supported by NSF grant EAR-9980551 awarded to C.L.-B. C.P.C. was supported by a fellowship from the David and Lucile Packard Foundation awarded to C.L.-B. S.B. was supported by an Alfred P. Sloan foundation fellowship awarded to C.L.-B. and a University of Michigan Turner Postdoctoral Fellowship. C.P.C. thanks the Danish Lithosphere Center in Copenhagen, Denmark and the Department of Earth and Planetary Sciences at Johns Hopkins University for hosting extended visits. We thank L. Ruff for insightful discussions on seismic coupling and M. Billen, S. King, S. Zhong, and an anonymous referee for comments that helped improve the manuscript. We thank M. Billen for the suggestion of including a flow chart in Fig. 6. [SK]

Appendix A

We use a genetic algorithm to invert for the fraction of the pull force that must be present at each subduction zone in order to minimize the misfit between the predicted and observed velocity fields. Genetic algorithms are directed random search methods that optimize the solution to potentially complicated inverse problems by analogy with the processes of natural selection and evolution [51,52]. Typically, a genetic algorithm operates using a population of about 100 possible solutions to the forward problem. Each of these 'individuals' in this population is initially randomly selected, but the frequency with which each individual is propagated into subsequent 'generations' is based on that individual's 'fitness', or its ability to minimize the misfit. With successive generations, the best-fitting solution improves because individuals that provide a better solution to a given problem are preferentially selected for reproduction into the next generation. Genetic algorithms have been shown to be capable of searching a large parameter space quickly and thoroughly, which makes them useful for this study.

We follow the method used by King [53] to invert for mantle viscosity. We use a population of 100 solutions, each of which is defined by a string of 40 binary digits, or four digits for each of the 10 subduction zones. These four digits describe a range of possible fractions of the maximum pull force (Fig. 1) between 0% (only slab suction) and 100% (only slab pull), with a resolution of 6.67%. The prescribed fraction of the maximum pull force (Table 1) is applied at each subduction zone. Whatever fraction of the excess slab weight that does not operate as pull is instead assumed to be supported by the viscous mantle, exciting slab suction. The plate motions that result from this set of plate-driving forces are calculated according to the method described in the text. The misfit between this solution and the observed plate motions is used to determine the fitness of each solution.

Individuals are propagated into successive generations according to tournament selection [53]. In this method, pairs of randomly selected indi-

viduals are compared based on their ability to minimize the misfit, with the more fit of the two individuals being promoted to the next generation in each case. To promote genetic diversity, individuals undergo ‘crossover’ at the start of each new generation. In this process, genetic material ahead of a randomly selected location on the binary string is switched with that of another individual. Additional genetic information is added by randomly switching individual bits in the binary strings with a ‘mutation’ rate of 0.4%. Finally, we retain the single best-fitting solution between generations to maintain continuity. The eventual best-fitting solution is typically achieved after about 200 generations, but we run our genetic algorithm for 300 generations for completeness.

References

- [1] B.H. Hager, Subducted slabs and the geoid: Constraints on mantle rheology and flow, *J. Geophys. Res.* 89 (1984) 6003–6015.
- [2] D. McKenzie, Speculations on the consequences and causes of plate motions, *Geophys. J. R. Astron. Soc.* 18 (1969) 1–32.
- [3] F. Richter, D. McKenzie, Simple plate models of mantle convection, *J. Geophys. Res.* 44 (1978) 441–471.
- [4] H. Bijwaard, W. Spakman, E.R. Engdahl, Closing the gap between regional and global travel time tomography, *J. Geophys. Res.* 103 (1998) 30055–30078.
- [5] S.P. Grand, R.D. van der Hilst, S. Widiyantoro, Global seismic tomography: A snapshot of convection in the Earth, *GSA Today* 7 (1997) 1–7.
- [6] R. van der Hilst, S. Widiyantoro, E.R. Engdahl, Evidence for deep mantle circulation from global tomography, *Nature* 386 (1997) 578–584.
- [7] D.L. Turcotte, E.R. Oxburgh, Finite amplitude convective cells and continental drift, *J. Fluid Mech.* 28 (1967) 29–42.
- [8] W.M. Chapple, T.E. Tullis, Evaluation of the forces that drive plates, *J. Geophys. Res.* 82 (1977) 1967–1984.
- [9] D. Forsyth, S. Uyeda, On the relative importance of the driving forces of plate motion, *Geophys. J. R. Astron. Soc.* 43 (1975) 163–200.
- [10] B.H. Hager, R.J. O’Connell, A simple global model of plate dynamics and mantle convection, *J. Geophys. Res.* 86 (1981) 4843–4867.
- [11] C. Lithgow-Bertelloni, M.A. Richards, The dynamics of Cenozoic and Mesozoic plate motions, *Rev. Geophys.* 36 (1998) 27–78.
- [12] S.C. Solomon, N.H. Sleep, Some simple physical models for absolute plate motions, *J. Geophys. Res.* 79 (1974) 2557–2567.
- [13] C.P. Conrad, C. Lithgow-Bertelloni, How mantle slabs drive plate tectonics, *Science* 298 (2002) 207–209.
- [14] T.W. Becker, R.J. O’Connell, Predicting plate motions with mantle circulation models, *Geochem. Geophys. Geosyst.* 2 (2001) 2001GC000171.
- [15] Y. Ricard, C. Vigny, Mantle dynamics with induced plate tectonics, *J. Geophys. Res.* 94 (1989) 17543–17559.
- [16] N.H. Sleep, M.N. Toksöz, Evolution of marginal basins, *Nature* 233 (1971) 548–550.
- [17] D.L. Kohlstedt, B. Evans, S.J. Mackwell, Strength of the lithosphere: Constraints imposed by laboratory experiments, *J. Geophys. Res.* 100 (1995) 17587–17602.
- [18] W.M. Elsasser, Convection and stress propagation in the upper mantle, in: S.K. Runcorn (Ed.), *The Application of Modern Physics to the Earth and Planetary Interiors*, Wiley-Interscience, London, 1969, pp. 223–246.
- [19] C. Christova, C.H. Scholz, Stresses in the Vanuatu subducting slab: A test of two hypotheses, *Geophys. Res. Lett.* 30 (2003) 2003GL017701.
- [20] E. Ito, H. Sato, Aseismicity in the lower mantle by superplasticity of the descending slab, *Nature* 351 (1991) 140–141.
- [21] J.X. Mitrovica, Haskell [1935] revisited, *J. Geophys. Res.* 101 (1996) 555–569.
- [22] L. Moresi, M. Gurnis, Constraints on the lateral strength of slabs from three-dimensional dynamic flow models, *Earth Planet. Sci. Lett.* 138 (1996) 15–28.
- [23] S. Zhong, G.F. Davies, Effects of plate and slab viscosities on the geoid, *Earth Planet. Sci. Lett.* 170 (1999) 487–496.
- [24] M.I. Billen, M. Gurnis, M. Simons, Multiscale dynamics of the Tonga-Kermadec subduction zone, *Geophys. J. Int.* 153 (2003) 359–388.
- [25] C.P. Conrad, B.H. Hager, Effects of plate bending and fault strength at subduction zones on plate dynamics, *J. Geophys. Res.* 104 (1999) 17551–17571.
- [26] T.B. Larsen, D.A. Yuen, A.V. Malevsky, Dynamical consequences on fast subducting slabs from a self-regulating mechanism due to viscous heating in variable viscosity convection, *Geophys. Res. Lett.* 22 (1995) 1277–1280.
- [27] J.F. Pacheco, L.R. Sykes, C.H. Scholz, Nature of seismic coupling along simple plate boundaries of the subduction type, *J. Geophys. Res.* 98 (1993) 14133–14159.
- [28] L. Ruff, H. Kanamori, Seismicity and the subduction process, *Phys. Earth Planet. Inter.* 23 (1980) 240–252.
- [29] S. Uyeda, H. Kanamori, Back-arc opening and the mode of subduction, *J. Geophys. Res.* 84 (1979) 1049–1061.
- [30] L.J. Ruff, Do trench sediments affect great earthquake occurrence in subduction zones?, *Pageoph* 129 (1989) 263–282.
- [31] J. Kelleher, W. McCann, Buoyant zones, great earthquakes, and unstable boundaries of subduction, *J. Geophys. Res.* 81 (1976) 4885–4896.
- [32] E.T. Peterson, T. Seno, Factors affecting seismic moment release rates in subduction zones, *J. Geophys. Res.* 89 (1984) 10233–10248.
- [33] C.H. Scholz, C. Small, The effect of seamount subduction on seismic coupling, *Geology* 25 (1997) 487–490.

- [34] T.-R.A. Song, M. Simons, Large trench-parallel gravity variations predict seismogenic behavior in subduction zones, *Science* 301 (2003) 630–633.
- [35] H. Kanamori, The energy release in great earthquakes, *J. Geophys. Res.* 82 (1977) 2981–2987.
- [36] Y. Ricard, M.A. Richards, C. Lithgow-Bertelloni, Y.L. Stunff, A geodynamical model of mantle density heterogeneity, *J. Geophys. Res.* 98 (1993) 21895–21909.
- [37] R.G. Gordon, D.M. Jurdy, Cenozoic global plate motions, *J. Geophys. Res.* 91 (1986) 12389–12406.
- [38] C. Lithgow-Bertelloni, M.A. Richards, Y. Ricard, R.J. O’Connell, D.C. Engebretson, Toroidal-poloidal partitioning of plate motion since 120 Ma, *Geophys. Res. Lett.* 20 (1993) 375–378.
- [39] C.E. Hall, M. Gurnis, M. Sdrolias, L.L. Lavier, R.D. Muller, Catastrophic initiation of subduction following forced convergence across fracture zones, *Earth Planet. Sci. Lett.* 212 (2003) 15–30.
- [40] M.A. Richards, C. Lithgow-Bertelloni, Plate motion changes, the Hawaiian-Emperor bend, and the apparent success and failure of geodynamic models, *Earth Planet. Sci. Lett.* 137 (1996) 19–27.
- [41] J.M. O’Connor, A.P. le Roex, South Atlantic hotspot-plume systems: 1. Distribution of volcanism in time and space, *Earth Planet. Sci. Lett.* 113 (1992) 343–364.
- [42] W.H. Press, B.P. Flannery, S.A. Teukolsky, W.T. Vetterling, *Numerical Recipes in Fortran*, Cambridge University Press, New York, 1992, 992 pp.
- [43] G.F. Sella, T.H. Dixon, A. Mao, REVEL: A model for recent plate velocities from space geodesy, *J. Geophys. Res.* 107 (2002) 2000JB000033.
- [44] A.M. Dziewonski, T.-A. Chou, J.H. Woodhouse, Determination of earthquake source parameters from waveform data for studies of global and regional seismicity, *Geophys. Res.* 86 (1981) 2825–2852.
- [45] R.D. Jarrard, Relations among subduction parameters, *Rev. Geophys.* 24 (1986) 217–284.
- [46] P. Bird, An updated digital model of plate boundaries, *Geochem. Geophys. Geosyst.* 3 (2003) 2001GC000252.
- [47] B. Pelletier, S. Calmant, R. Pillet, Current tectonics of the Tonga-New Hebrides region, *Earth Planet. Sci. Lett.* 164 (1998) 263–276.
- [48] C.P. Conrad, B.H. Hager, Mantle convection with strong subduction zones, *Geophys. J. Int.* 144 (2001) 271–288.
- [49] B.H. Hager, R.J. O’Connell, Subduction zone dip angles and flow driven by plate motion, *Tectonophysics* 50 (1978) 111–133.
- [50] S.D. King, J.P. Lowman, C.W. Gable, Episodic tectonic plate reorganizations driven by mantle convection, *Earth Planet. Sci. Lett.* 203 (2002) 83–91.
- [51] S. Forrest, Genetic algorithms Principles of natural selection applied to computation, *Science* 261 (1993) 872–878.
- [52] D.E. Goldberg, *Genetic Algorithms in Search, Optimization and Machine Learning*, Addison-Wesley, Reading, MA, 1989, 432 pp.
- [53] S.D. King, Radial models of mantle viscosity: results from a genetic algorithm, *Geophys. J. Int.* 122 (1995) 725–734.